

Original Article

# Influence of Channel Estimation Error in a Multiuser TAS/MRC Scheme Subject to Beaulieu-Xie Fading Channels

Amardeep Kumar Thakur<sup>1</sup>, Rajkishur Mudoi<sup>2</sup>, Rupaban Subadar<sup>3</sup>

<sup>1,2,3</sup>Department of Electronics and Communication Engineering, North-Eastern Hill University, Meghalaya, India.

<sup>2</sup>Corresponding Author : [rajkishur@gmail.com](mailto:rajkishur@gmail.com)

Received: 17 July 2025

Revised: 17 August 2025

Accepted: 16 September 2025

Published: 30 September 2025

**Abstract** - The Transmit Antenna Selection incorporating Maximal Ratio Combining (TAS/MRC) strategy is a broadly preferred approach to lessen the intricacy level of a multiuser system incorporating Multiple Input and Multiple Output (MIMO) technique with little degradation in the performance. Reducing RF links upgrades the practical suitability of the TAS/MRC strategy. In TAS/MRC communication, the Channel State Information (CSI) is presented to the transmitter. Depending on the CSI, the best antenna is chosen for transmission, thereby enhancing the system performance. However, due to the existence of dominant factors, namely the channel estimation error and the channel fading, the status of the TAS/MRC system may be reduced significantly. For the evaluation of the TAS/MRC strategy, it is commonly assumed that the lossless and error-free CSI is applied to the base station. However, practically, the CSI has envelope and phase errors; therefore, the error associated with the CSI needs to be applied in the system evaluation. Likewise, the functioning of the MRC receiver is influenced noticeably by the channel fading conditions. In this paper, a TAS/MRC scheme associated with multiple users has been analyzed. The channel estimation error and Beaulieu-Xie fading model are utilized for the mathematical evaluation of the system. In the reality of channel estimation error, the outage probability, ABER with BPSK as well as DBPSK modulations, and ergodic capacity have been derived and analyzed. It can be noticed that little envelope errors in CSI may deteriorate the status of the system to a large extent when compared with the error in the phase of the CSI. Simulated points are included in the figures to validate the data.

**Keywords** - Beaulieu-Xie fading, DBPSK, Ergodic capacity, Multiuser MIMO, CSI, TAS/MRC.

## 1. Introduction

The MIMO is a favorable system to avoid the effect of fading as it produces both multiplexing and diversity gain [1]. However, MIMO is not desirable for multiuser environments due to the huge quantity of RF links, which leads to the initiation of a new variation of MIMO with the Transmit Antenna Selection (TAS) algorithm. The TAS system decreases the complexity of the conventional MIMO system by reducing the quantity of RF links and easily selecting the best antenna for communication. The TAS algorithm needs the information of the CSI to select the best antenna for communication. With the TAS algorithm, the receiver may use MRC; thereby, the system is known as a TAS/MRC system [2], and the execution of the aforesaid system is comparable to the regular MIMO system with less complexity [3, 4]. Due to its applicability in the multiuser wireless environment, the TAS/MRC system gets attention from researchers, and several works have been published on the analysis of this system in the Rayleigh and Nakagami- $m$  fading environments. In [5], an MRC user performance under

a correlated Nakagami-fading model is investigated. In [6], the Average Bit-Error Rate (ABER) of TAS adding receive MRC is evaluated in Rayleigh statistical channels. In [7], the error condition of a TAS scheme combining receiver MRC is investigated for Nakagami- $m$  fading distributions. In [8], the TAS/MRC system performance for correlated Nakagami fading channels is evaluated to minimize the complexity of communication and maintain the diversity benefit. In [9], the ABER of an MRC user with TAS at the transmitter is presented for Nakagami- $m$  fading channels. The Nakagami- $m$  adjusts the number of multipath clusters by varying  $m$  [10]. The Rician fading model is more appropriate whenever Line-Of-Sight (LOS) or established components are available in the wireless medium [11]. Merging the usefulness of the aforesaid two models, Beaulieu and Xie suggested a modern Beaulieu-Xie fading distribution [12], which exhibits both specular as well as diffuse scattering components, thereby making it suitable for both LOS as well as non-LOS layouts [13]. The model is usually applicable for shaping the fading distribution of heterogeneous arrangements, femtocells, and



high-speed trains [14]. In [15], the Level Crossing Rate (LCR) as well as Average Fade Duration (AFD) of the MRC type diversity receiver in the Beaulieu-Xie fading environment are studied. In [16], the effective capacity under the Beaulieu-Xie distribution is analysed. In [17], the analysis of the transmission system inside the femtocells in relation to MRC diversity and Beaulieu-Xie fading distribution is performed. In [18], the effective rate evaluation for a Multiple Input Single Output (MISO) scheme under the Beaulieu-Xie distribution is presented. In [19], the physical layer security of the wireless transmission scheme incorporating a wiretap channel and a Reconfigurable Intelligent Surface (RIS) in the Beaulieu-Xie model has been studied. In [20], the Outage Probability (OP) for Selection Combining (SC) beneficiary considering Beaulieu-Xie distribution and the reaction of Co-Channel Interference (CCI) utilizing Rayleigh fading are examined. In [21], the performance of transmission OP and average harvested energy of wireless-powered systems for the Beaulieu-Xie distribution is analyzed. In [22], a new TAS technique incorporating the priority-based genetic algorithm, thereby generating an antenna subset with low complexity, is introduced. In [23], the status of a MIMO system applying short-packet communication and TAS/SC over a Rayleigh distribution is examined. In [24], the execution of a TAS adding MRC technique for an unmanned aerial vehicle network over Nakagami- $m$  channel is investigated.

After meticulously observing the literature, it is found that very few publications are available on TAS/MRC with channel estimation errors. Since this is a practical issue and exists in the real system, the analysis is performed considering the effect before the installation of such a system. However, no literature on channel estimation errors or Beaulieu-Xie fading channels can be found. The primary augmentations and the novelty of this work can be outlined below:

- The joint CDF of all the links, considering channel estimation error and Beaulieu-Xie fading distribution, is obtained.
- The PDF for the SNR regarding the multiuser TAS/MRC scheme applying channel estimation error is derived.
- The OP of the transmission strategy is realized and analyzed in terms of the 1st-order Laguerre Polynomial.
- The ABER applying coherent as well as non-coherent modulation techniques for the aforesaid system is derived and analyzed with regard to Appell hypergeometric function.
- The ergodic capacity regarding the multiuser TAS/MRC technique with channel estimation error and Beaulieu-Xie fading distribution is analyzed.

The succeeding segments of the paper are arranged as mentioned. In sector 2, the channels and communication model explanation are reflected. The OP analysis of the

multiuser TAS/MRC method, the ABER analysis and the ergodic capacity evaluation are framed in division 3, division 4 and division 5, respectively. In portion 6, the outcomes and descriptions are mentioned. Finally, concluding comments are given in segment 7.

## 2. System and Channel Pattern Description

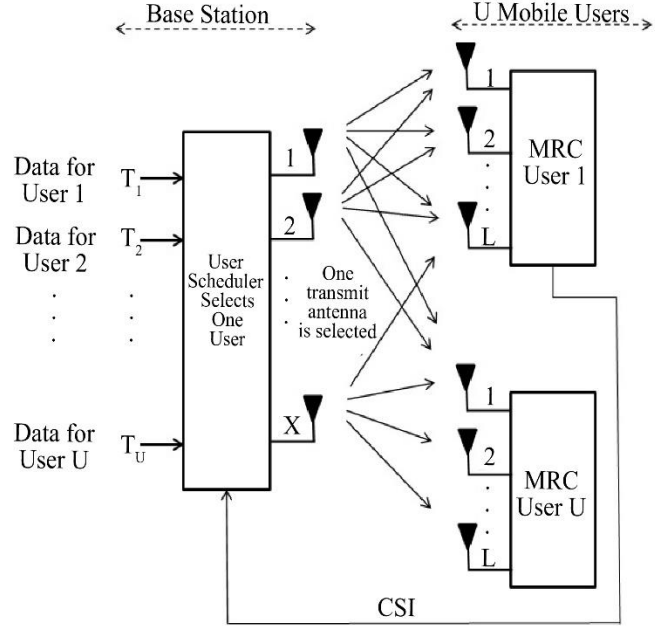


Fig. 1 The multiuser TAS/MRC block diagram

A multiuser MIMO system applying TAS/MRC, as depicted in Figure 1, is studied in this work for the estimation of downlink data transmission. At the base station, the system uses  $A$  number of transmit antennas. The transmit antennas are represented by  $A \in \{1, 2, \dots, X\}$ . The base station serves  $U$  ( $U \leq X$ ) users, and  $L$  (from  $1, 2, \dots, L$ ) receive antennas are associated with each user. A user is offered a particular antenna at the base station to send the data to  $T_U$ . Again,  $U$  describes the user number (from  $1, 2, \dots, U$ ). The channel between the transmit antenna  $A$  and the received antennas experiences a flat Beaulieu-Xie fading model. The CSI is provided to the base station with a feedback path, depending on which antenna is chosen for downlink transmission. The complex low-pass correspondent of the signal acquired by the  $L$ th antenna of the user for a bit duration  $T_b$  may be given as:

$$r_L(t) = \alpha_L e^{j\phi_L} z(t) + n_L(t), 0 \leq t \leq T_b. \quad (1)$$

Whereby  $z(t)$  represents the signal of the sent bit having energy  $E_b$ , as well as  $n_L$  the Gaussian noise with zero mean, and the two-part power spectral density  $2N_0$ . Random Variable (RV)  $\phi_L$  denotes the phase, which is uniformly dispersed in a range  $[0, 2\pi]$  and  $\alpha_L$  indicates the Beaulieu-Xie category fading envelope. The instantaneous SNR at the  $L$ th antenna of a user,  $\gamma_L = \frac{E_b}{N_0} \alpha_L^2$ , whose PDF is stated as [16]:

$$f_{\gamma_L}(\gamma_L) = \sqrt{\frac{\eta^{m+1}\gamma_L^{m-1}}{(mk)^{m-1}}} \exp(-mk - \eta\gamma_L) I_{m-1}(2\sqrt{mk\eta\gamma_L}) \quad (2)$$

Where  $k$  is the ratio of specular power to the diffuse power components  $k = \frac{\lambda^2}{\Omega}$ ,  $\lambda$  it influences the location and height of the PDF mode, and  $\Omega$  regulates its spread.  $\eta = \frac{L_1^{m-1}(-mk)}{\bar{\gamma}}$ ,  $\bar{\gamma}$  is the average received SNR on the  $L$ th branch,  $L_w^\partial(\cdot)$  represents the  $w$ th-order Laguerre Polynomial, and  $m$  denotes the severity of fading. Function  $I_x(\cdot)$  denotes the first kind of modified Bessel's function of order  $x$ . Rayleigh fading is the special case of this fading whenever  $m=1$ ,  $k=0$ , and it also simplifies to the Rician distribution whenever  $m=1$  and for each value of  $k$ .

Each user of the transmission structure carries out MRC to improve the condition of the downlink data. In the case of the MRC diversity, the collected data from all received antennas of a user are co-phased, amplified by a weight factor proportional to the individual input SNR and summed to improve the output SNR. For the MRC user, the instantaneous output SNR  $\gamma$  incorporating the channel estimation error can be yielded as [25],

$$\gamma_{occe} = B \sum_{i=1}^L \gamma_i, \quad (3)$$

whereby  $\gamma_i$  stands for the instantaneous SNR of the  $i^{th}$  branch, along with  $L$ , which denotes the number of input antennas in the MRC receiver. In (3),  $B = \frac{|p|^2 \cos^2(\Delta\theta)}{(1-|p|^2)\bar{\gamma}_L+1}$  [26, 27]. Here  $|p|$  is the error in envelope detection, and  $\Delta\theta$  is the phase error. The CSI of each user has been provided to the base station with the help of a feedback path having channel estimation errors, based on which the scheduler allocates the finest antenna to each user. Utilizing the characteristic function-based approach of (2), the PDF of SNR on the output of an MRC receiver is expressed as [17]:

$$f_\gamma(\gamma) = \frac{\eta^{mL}}{\Gamma(mL)} \exp(-(mkL + \eta\gamma)) \times \gamma^{mL-1} {}_0F_1(; mL; m k L \eta \gamma) \quad (4)$$

Whereby,  $\Gamma(\cdot)$  and  ${}_0F_1(; \cdot; \cdot)$  symbolize the gamma function and confluent hypergeometric function, respectively. Doing RV transformation, for an MRC receiver, the PDF for the output SNR with channel estimation error is yielded as

$$f_{\gamma_{occe}}(\gamma) = \frac{\eta^{mL}}{B\{\Gamma(mL)\}} \exp\left(-\left(mkL + \eta\frac{\gamma}{B}\right)\right) \times \left(\frac{\gamma}{B}\right)^{mL-1} {}_0F_1(; mL; m k L \eta \frac{\gamma}{B}) \quad (5)$$

From (5), the CDF of the RV  $\gamma_{occe}$  is obtained as

$$F_{\gamma_{occe}}(\gamma) = \frac{\eta^{mL} \exp(-mkL)}{B^{mL}\{\Gamma(mL)\}} \times \int_0^\gamma \gamma^{mL-1} \exp\left(-\eta\frac{\gamma}{B}\right) {}_0F_1(; mL; m k L \eta \frac{\gamma}{B}) d\gamma \quad (6)$$

Expanding the function  ${}_0F_1(; \cdot; \cdot)$  in the infinite series, one can write,

$$F_{\gamma_{occe}}(\gamma) = \frac{\eta^{mL} \exp(-mkL)}{B^{mL}\{\Gamma(mL)\}} \sum_{t=0}^{\infty} \frac{(mkL \eta \frac{1}{B})^t}{t!(mL)_t} \times \int_0^\gamma \gamma^{mL+t-1} \exp\left(-\eta\frac{\gamma}{B}\right) d\gamma \quad (7)$$

Applying [28, (3.381.1)] in (7),

$$F_{\gamma_{occe}}(\gamma) = \exp(-mkL) \times \sum_{t=0}^{\infty} \frac{(mkL)^t}{t!\Gamma(mL+t)} g\left(mL + t, \eta\frac{\gamma}{B}\right) \quad (8)$$

Where,  $g(\vartheta, \rho) = \int_0^\rho \Delta^{\vartheta-1} e^{-\Delta} d\Delta$  represents the lower incomplete gamma function. The total  $X$  transmit antennas are associated with the base station, and for  $U$  quantity of users, the total communication links will be  $XU$ .

The CDF statement of each of the links is stated in (8). For all the links, the joint CDF can be obtained as

$$F_{\gamma_{Mcee}}(\gamma) = [\exp(-mkL) \times \sum_{t=0}^{\infty} \frac{(mkL)^t}{t!\Gamma(mL+t)} g\left(mL + t, \eta\frac{\gamma}{B}\right)]^{XU} \quad (9)$$

In case of the multiuser TAS/MRC strategy, the PDF as regards the output SNR is derived from (9) as

$$f_{\gamma_{Mcsi}}(\gamma) = XU [\exp(-mkL)]^{XU} \times \sum_{t_1=0}^{\infty} \sum_{t_2=0}^{\infty} \dots \sum_{t_{XU-1}=0}^{\infty} \frac{(mkL)^{\sum_{i=1}^{XU} t_i}}{\prod_{i=1}^{XU} t_i! \Gamma(mL+t_i)} \times \left[ g\left(mL + t, \eta\frac{\gamma}{B}\right) \right]^{XU-1} \times \sum_{t=0}^{\infty} \frac{(mkL)^t}{t!\Gamma(mL+t)} \frac{d}{d\gamma} g\left(mL + t, \eta\frac{\gamma}{B}\right) \quad (10)$$

Simplifying with the help of [29, (6.5.25)] and thereafter replacing  $g(\cdot, \cdot)$  with [30, (1.7)], the output SNR PDF concerning the system can be yielded as

$$\begin{aligned}
 f_{\gamma_{Mcsi}}(\gamma) &= XU e^{-mkLXU} \\
 &\times \sum_{i=1,2,\dots,XU}^{\infty} t_i=0 \sum_{j=0,1,\dots,XU-1}^{\infty} v_j=0 \frac{(mkL)^{\sum_{i=1}^{XU} t_i} \left(\frac{\eta}{B}\right)^{mLXU + \sum_{i=1}^{XU} t_i + \sum_{j=1}^{XU-1} v_j}}{\{\prod_{i=1}^{XU} t_i! \Gamma(mL + t_i)\}} \\
 &\times \frac{e^{-\frac{\eta XU}{B} \gamma} \gamma^{mLXU + \sum_{i=1}^{XU} t_i + \sum_{j=1}^{XU-1} v_j - 1}}{\{\prod_{i=1}^{XU-1} \prod_{j=1}^{XU-1} (mL + t_i) v_{j+1}\}} \quad (11)
 \end{aligned}$$

### 3. Outage Probability Analysis

Outage probability  $P_{Ocsi}$  signifies that the possibility of spontaneous error goes beyond a distinct level [5]. The SNR goes under a defined threshold  $\gamma_{th}$  [25]. The OP shows an elementary performance benchmark of the quality of service for mobile communication models [31]. From (9), the statement of OP for the multiuser TAS/MRC scheme with channel estimation error is written as

$$\begin{aligned}
 P_{Ocsi} &= [\exp(-mkL) \\
 &\times \sum_{t=0}^{\infty} \frac{(mkL)^t}{t! \Gamma(mL + t)} g\left(mL + t, \eta \frac{\gamma_{th}}{B}\right)]^{XU} \quad (12)
 \end{aligned}$$

It may also be written as

$$\begin{aligned}
 P_{Ocsi} &= [\exp(-mkL) \\
 &\times \sum_{t=0}^{\infty} \frac{(mkL)^t}{t! \Gamma(mL + t)} g\left(mL + t, \frac{L_1^{m-1}(-mk)}{\bar{\gamma}_N B}\right)]^{XU} \quad (13)
 \end{aligned}$$

where  $\bar{\gamma}_N = \frac{\bar{\gamma}}{\gamma_{th}}$  interprets the normalized SNR for each branch.

### 4. Average Bit Error Rate Analysis

The ABER of a wireless transmission model for different modulation patterns may be evaluated by averaging the CDF of the SNR over the derivative of the Conditional Error Probability (CEP) for the modulation technique applied [32]. It is expressed as

$$\bar{p}_e = - \int_0^{\infty} p_e'(\gamma) F_{\gamma}(\gamma) d\gamma \quad (14)$$

Whereby,  $p_e'(\gamma)$  is the derivative of the CEP and is written as [32]:

$$p_e'(\gamma) = \frac{-\alpha^{\varpi} \gamma^{\varpi-1} e^{-\alpha\gamma}}{2\Gamma(\varpi)} \quad (15)$$

Where, for a few binary modulations, the number of parameters  $\alpha$  and  $\varpi$  are [32]:  $(\alpha, \varpi) = (1, 0.5)$  for BPSK and  $(\alpha, \varpi) = (1, 1)$  for DBPSK. Inserting the values of  $F_{\gamma}(\gamma)$  and  $p_e'(\gamma)$  from (9) and (15) into (14), respectively and

applying [29, (6.5.12)],  $g(\dots)$  is replaced by a hypergeometric function as,

$$\begin{aligned}
 \bar{p}_e &= \frac{\alpha^{\varpi} e^{-mkLXU}}{2\Gamma(\varpi)} \\
 &\times \sum_{t_1=0}^{\infty} \sum_{t_2=0}^{\infty} \dots \sum_{t_{XU}=0}^{\infty} \frac{(mkL)^{\sum_{i=1}^{XU} t_i} \left(\frac{\eta}{B}\right)^{mLXU + \sum_{i=1}^{XU} t_i}}{\prod_{i=1}^{XU} (mL + t_i) t_i! \Gamma(mL + t_i)} \\
 &\times \int_0^{\infty} e^{-\left(\alpha + \frac{\eta XU}{B}\right) \gamma} \gamma^{mLXU + \sum_{i=1}^{XU} t_i + \varpi - 1} \\
 &\times \left[ \prod_{i=1}^{XU} {}_1F_1\left(1, 1 + mL + t_i, \eta \frac{\gamma}{B}\right) \right] d\gamma \quad (16)
 \end{aligned}$$

Solving the integral with the help of the expression [33, (C.1)], the ABER can be obtained as

$$\begin{aligned}
 \bar{p}_e &= \frac{\alpha^{\varpi} e^{-mkLXU}}{2\Gamma(\varpi)} \\
 &\times \sum_{t_1=0}^{\infty} \sum_{t_2=0}^{\infty} \dots \sum_{t_{XU}=0}^{\infty} \frac{(mkL)^{\sum_{i=1}^{XU} t_i} \left(\frac{\eta}{B}\right)^{mLXU + \sum_{i=1}^{XU} t_i}}{\prod_{i=1}^{XU} (mL + t_i) t_i! \Gamma(mL + t_i)} \\
 &\times \left(\alpha + \frac{\eta XU}{B}\right)^{-(mLXU + \sum_{i=1}^{XU} t_i + \varpi)} \\
 &\times \Gamma(mLXU + \sum_{i=1}^{XU} t_i + \varpi) \\
 &\times F_A\left(mLXU + \sum_{i=1}^{XU} t_i + \varpi; 1, \dots, 1; \right. \\
 &\quad \left. \frac{1 + mL + t_1, \dots, 1 + mL + t_{XU}}{XU, times}; \right. \\
 &\quad \left. \frac{\eta}{\alpha B + \eta XU}, \dots, \frac{\eta}{\alpha B + \eta XU} \right) \quad (17)
 \end{aligned}$$

Where  $F_A(\dots; \dots; \dots)$  is the Appell hypergeometric function.

### 5. Ergodic Capacity Analysis

For the channel with receiver CSI, the ergodic capacity could be stated from [34] as,

$$C_{csi} = H \int_0^{\infty} \log_2(1 + \gamma) f_{\gamma_{Mcsi}}(\gamma) d\gamma \quad (18)$$

whereby  $H$  is the channel bandwidth. Putting the expression of (11) into (18), the ergodic capacity of the channel is expressed as

$$C_{csi} = H \log_2(e) XU e^{-mkLXU}$$

$$\begin{aligned}
 & \times \sum_{i=1,2,\dots,XU}^{\infty} t_i=0 \sum_{j=0,1,\dots,XU-1}^{\infty} v_j=0 \frac{(mkL)^{\sum_{i=1}^{XU} t_i}}{\{\prod_{i=1}^{XU} t_i! \Gamma(mL+t_i)\}} \\
 & \times \frac{\left(\frac{\eta}{B}\right)^{mLXU+\sum_{i=1}^{XU} t_i+\sum_{j=1}^{XU-1} v_j}}{\{\prod_{i=1}^{XU-1} \prod_{j=1}^{XU-1} (mL+t_i) v_{j+1}\}} \\
 & \times \int_0^{\infty} \ln(1+\gamma) e^{-\frac{\eta XU}{B} \gamma} (\gamma)^{mLXU+\sum_{i=1}^{XU} t_i+\sum_{j=1}^{XU-1} v_{j+1}-1} d\gamma
 \end{aligned} \quad (19)$$

Simplifying,

$$\begin{aligned}
 C_{csi} &= H \log_2(e) XU e^{-mkLXU} \\
 & \times \sum_{i=1,2,\dots,XU}^{\infty} t_i=0 \sum_{j=0,1,\dots,XU-1}^{\infty} v_j=0 \frac{(mkL)^{\sum_{i=1}^{XU} t_i}}{\{\prod_{i=1}^{XU} t_i! \Gamma(mL+t_i)\}} \\
 & \times \frac{\left(\frac{\eta}{B}\right)^{mLXU+\sum_{i=1}^{XU} t_i+\sum_{j=1}^{XU-1} v_j}}{\{\prod_{i=1}^{XU-1} \prod_{j=1}^{XU-1} (mL+t_i) v_{j+1}\}} \\
 & \times I_{mLXU+\sum_{i=1}^{XU} t_i+\sum_{j=1}^{XU-1} v_j} \left(\frac{\eta XU}{B}\right)
 \end{aligned} \quad (20)$$

Where  $I_{\xi}(v) = \int_0^{\infty} \phi^{\xi-1} \ln(1+\phi) e^{-v\phi} d\phi$ . For an integer  $\xi$ , a function  $I_{\xi}(v)$  may be expressed as  $I_{\xi}(v) = (\xi-1)! e^v \sum_{h=1}^{\xi} \frac{\Gamma(-\xi+h, v)}{v^h}$  [35].

## 6. Numerical Outcomes and Discussion

The analytical statements of outage probability, ABER, and ergodic capacity have been calculated and illustrated. The data are illustrated for arbitrary numerals of the diversity order  $L$ , an arbitrary number of users  $U$  and a fading parameter  $m$  taking different levels of  $k$ . In Figure 2,  $P_{Ocsi}$  vs.  $\bar{\gamma}$  is depicted for divergent numbers of  $k, L$ , and  $m$ . In Figure 2,  $|p| = 0.97$  and  $\Delta\theta = \pi/20$  generate the channel estimation error. The threshold SNR is taken as  $\gamma_{th} = 2dB$ .

For evaluation,  $X=2$  and  $U=2$  are considered. With the increment in  $k$  and  $m$ , the receiver undergoes less outage for a specified amount of  $\gamma_{th}$ . The outage performance rises with an increment in  $L$  and  $m$ . It is noticed that with  $L=2, k=3$  and  $m=2$ , the OP performance enhances after 9 dB compared to  $L=4, m=1$  and  $k=1$ . This means that a higher  $L$  has less impact on the system than a higher  $k$  and  $m$ , which is a higher average SNR for each branch.

In Figure 3,  $P_{Ocsi}$  Vs.  $\bar{\gamma}$  has been shown for varying values of  $m, |p|$  and  $\Delta\theta$  with  $X=2, L=2, U=2, k=3$  in the system. It  $\gamma_{th}$  is considered to be 2 dB. The outage performance improves with a decrease in  $\Delta\theta$  and is better at no phase error  $\Delta\theta = 0$ . Similarly, the receiver experiences

more outages for  $|p| = 0.97$  as compared to no envelope error  $|p| = 1$ . As expected, outage performance develops with an enhancement in  $m$ , which signifies better channels. In Figure 4, ABER vs.  $\bar{\gamma}$  has been illustrated for BPSK modulation considering arbitrary amounts of  $L, k$  and  $m$  with  $X=2, U=2$  in the system.

In Figure 4,  $|p| = 0.97$  and  $\Delta\theta = \pi/20$  are the channel estimation errors. As it is envisaged, ABER decreases with an increment in  $L, k$  and  $m$ . It is realized that ABER performance is better for  $L=2, k=3$  and  $m=2$  than  $L=4, k=1$  and  $m=1$  at low  $\bar{\gamma}$ . The increasing number of  $L$  on each user has less impact on ABER at low,  $\bar{\gamma}$  values related to the enhancement in  $k$  and  $m$ .

In Figure 5, ABER vs.  $\bar{\gamma}$  has been observed for DBPSK modulation considering divergent numbers of  $L, k$  and  $m$  incorporating  $X=2, U=2$ . In Figure 5, uniform execution is observed as in Figure 4. In Figure 6, ABER vs.  $\bar{\gamma}$  has been depicted for BPSK modulation by applying different numbers of  $U$  with  $X=2, L=2, k=3$  and  $m=1$ . The ABER performance is better, i.e., the ABER decreases with an increase  $\Delta\theta$ .

The ABER of the system is more for  $|p| = 0.97$  as compared to  $|p| = 1$ . The ABER performance upgrades with an increase in  $U$ . The results found by evaluating the derived equations are established by Monte Carlo simulations. From Figures 2 to 6, the simulated points are in close agreement.

Figure 7 shows the consequence of channel estimation error on ergodic capacity with  $X=2, L=2, U=2, m=1$ , and  $k=1$  in the system. It is seen that, for a relatively low value of  $\Delta\theta$ , the ergodic capacity increases. Similarly,  $|p| = 1$ , this results in an increase in capacity over that  $|p| = 0.97$  of the entire  $\bar{\gamma}$  system.

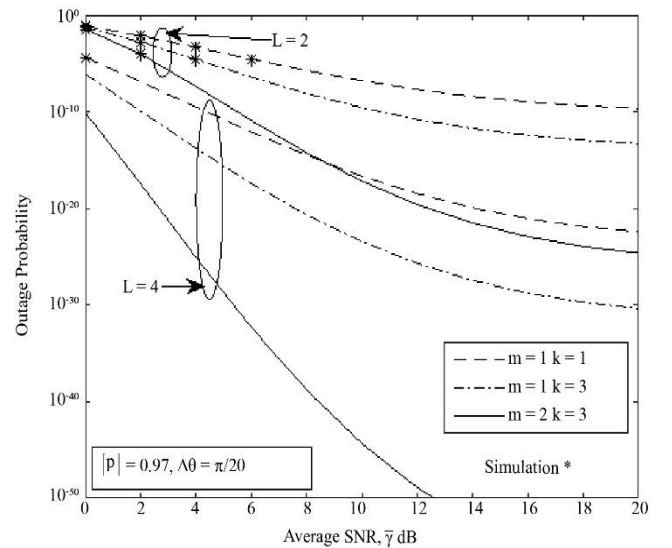


Fig. 2 OP vs. Average SNR per received antenna with  $X=2, U=2$

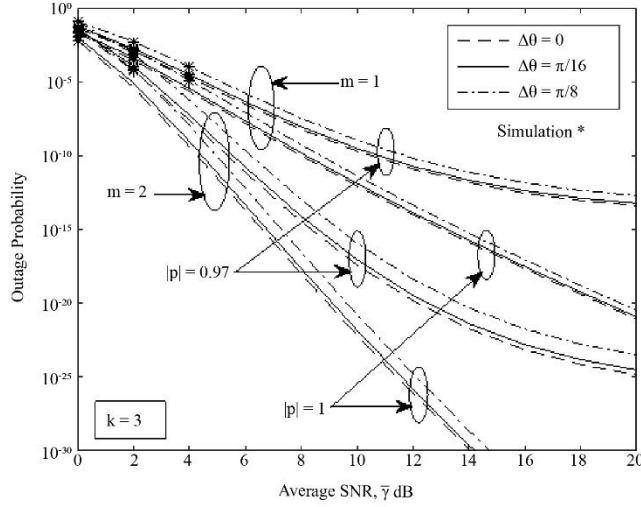


Fig. 3 OP vs. Average SNR per received antenna with  $X=2, L=2, U=2, k=3$ .

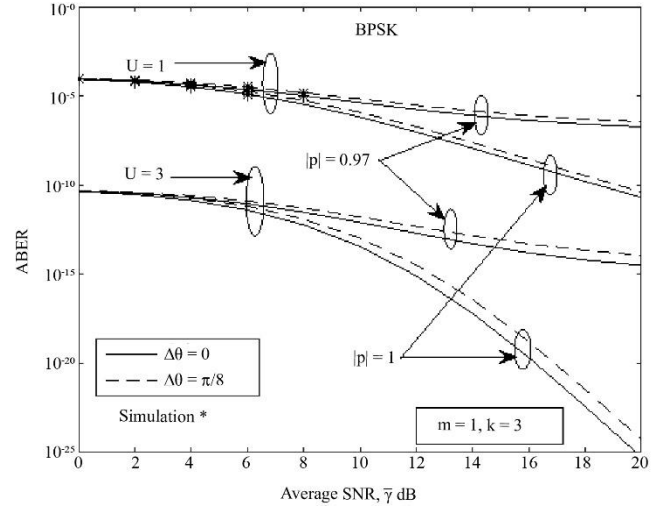


Fig. 6 ABER vs. Average SNR of BPSK modulation for  $X=2, L=2, k=3$  and  $m=1$ .

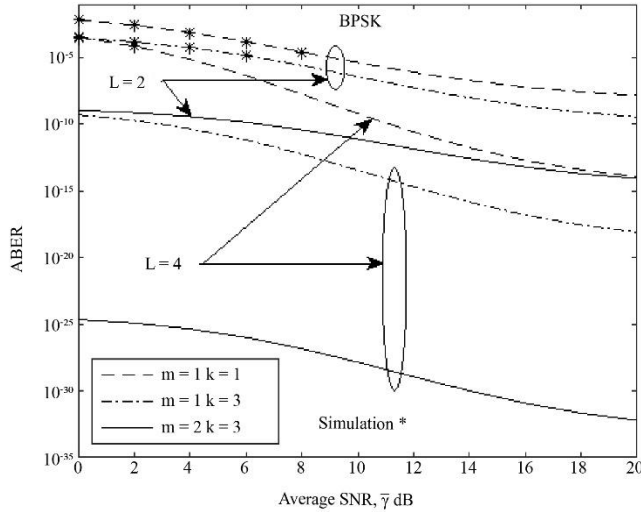


Fig. 4 ABER of BPSK modulation technique for  $X=2, U=2$ .

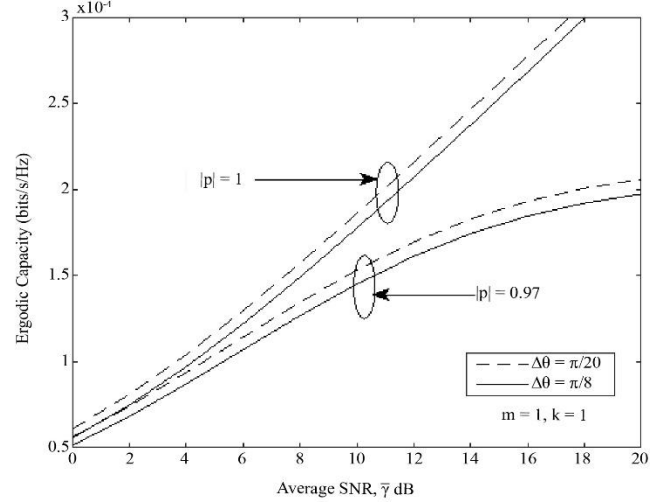


Fig. 7 Ergodic capacity vs. average SNR per received antenna,  $X=2, L=2, U=2, m=1$ , and  $k=1$ .

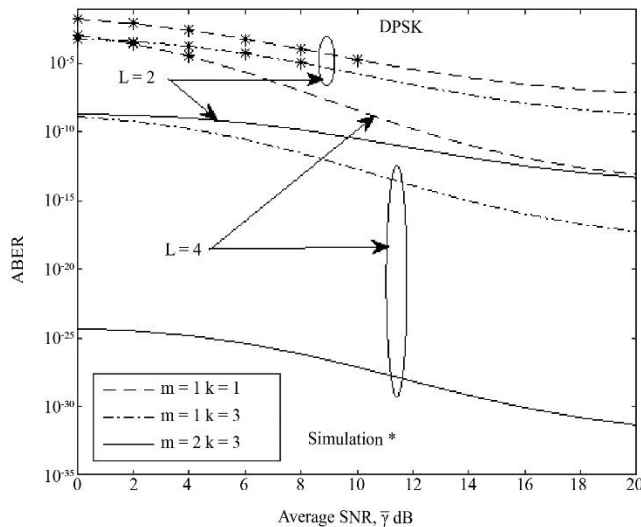


Fig. 5 ABER of DBPSK modulation technique for  $X=2, U=2$

## 7. Conclusion

The execution of the multiuser TAS/MRC technique is presented in this work, considering the channel estimation error as well as channel fading. The OP, ABER and ergodic capacity influenced by Beaulieu-Xie fading channels have been presented. The OP and ABER expressions are achieved with regard to the lower incomplete Gamma function and Appell hypergeometric function, respectively.

Ergodic capacity is found in relation to the Gamma function. Mathematically evaluated results and Monte Carlo simulated data have been depicted in the figures. Results reflect that the functioning of the system improves as an increment in diversity order, fading parameter, and the ratio of specular power to the diffuse power components of the channel. With an enhancement of the users, the ABER performance gets better. The error on the phase and the

envelope in the signal deteriorates the functioning of the communication pattern. The channel estimation error hurts the receiver's performance. In this communication structure,

the number of users is taken to be a maximum of three. Whenever the number of users increases, the number of RF links increases, and the system complexity increases.

## References

- [1] D. Gesbert et al., "Outdoor MIMO Wireless Channels: Models and Performance Prediction," *IEEE Transactions on Communications*, vol. 50, no.12, pp. 1926-1934, 2002. [[CrossRef](#)] [[Google Scholar](#)] [[Publisher Link](#)]
- [2] Zhuo Chen, Jinhong Yuan, and B. Vucetic, "Analysis of Transmit Antenna Selection / Maximal-Ratio Combining in Rayleigh Fading Channels," *IEEE Transactions on Vehicular Technology*, vol. 54, no. 4, pp. 1312-1321, 2005. [[CrossRef](#)] [[Google Scholar](#)] [[Publisher Link](#)]
- [3] Molisch Andreas F., and Moe Z. Win, "MIMO Systems with Antenna Selection," *IEEE Microwave Magazine*, vol. 5, no. 1, pp. 46-56, 2004. [[CrossRef](#)] [[Google Scholar](#)] [[Publisher Link](#)]
- [4] Qing Yan, and R.S. Blum, "Improved Space-Time Convolutional Codes for Quasi-Static Slow Fading Channels," *IEEE Transactions on Wireless Communications*, vol. 1, no. 4, pp. 563-71, 2002. [[CrossRef](#)] [[Google Scholar](#)] [[Publisher Link](#)]
- [5] V.A. Aalo, "Performance of Maximal-Ratio Diversity Systems in a Correlated Nakagami-Fading Environment," *IEEE Transactions on Communications*, vol. 43, no. 8, pp. 2360-2369, 1995. [[CrossRef](#)] [[Google Scholar](#)] [[Publisher Link](#)]
- [6] S. Thoen et al., "Performance Analysis of Combined Transmit-SC / Receive-MRC," *IEEE Transactions on Communications*, vol. 49, no. 1, pp. 5-8, 2001. [[CrossRef](#)] [[Google Scholar](#)] [[Publisher Link](#)]
- [7] Zhuo Chen, Zhanjiang Chi, and Branka Vucetic, "Error Performance of Maximal Ratio Combining with Transmit Antenna Selection in Nakagami- $m$  Fading Channels," *2006 International Conference on Wireless Communications, Networking and Mobile Computing*, Wuhan, China, pp. 1-3, 2006. [[CrossRef](#)] [[Google Scholar](#)] [[Publisher Link](#)]
- [8] Bao-Yun Wang, "Accurate BER of Transmitter Antenna Selection / Receiver-MRC Over Arbitrarily Correlated Nakagami Fading Channels," *2006 IEEE International Conference on Acoustics Speech and Signal Processing Proceedings*, Toulouse, France, vol. 4, 2006. [[CrossRef](#)] [[Google Scholar](#)] [[Publisher Link](#)]
- [9] Juan M. Romero-Jerez, and Andrea J. Goldsmith, "Performance of Multichannel Reception with Transmit Antenna Selection in Arbitrarily Distributed Nakagami Fading Channels," *IEEE Transactions on Wireless Communications*, vol. 8, no. 4, pp. 2006-2013, 2009. [[CrossRef](#)] [[Google Scholar](#)] [[Publisher Link](#)]
- [10] G.K. Karagiannidis, D.A. Zogas, and S.A. Kotsopoulos, "On the Multivariate Nakagami- $m$  Distribution with Exponential Correlation," *IEEE Transactions on Communications*, vol. 51, no. 8, pp. 1240-1244, 2003. [[CrossRef](#)] [[Google Scholar](#)] [[Publisher Link](#)]
- [11] A. Glavieux, P.Y. Cochet, and A. Picart, "Orthogonal Frequency Division Multiplexing with BFSK Modulation in Frequency Selective Rayleigh and Rician Fading Channels," *IEEE Transactions on Communications*, vol. 42, no. 234, pp. 1919-1928, 1994. [[CrossRef](#)] [[Google Scholar](#)] [[Publisher Link](#)]
- [12] Norman C. Beaulieu, and Xie Jiandong, "A Novel Fading Model for Channels with Multiple Dominant Specular Components," *IEEE Wireless Communications Letters*, vol. 4, no. 1, pp. 54-57, 2015. [[CrossRef](#)] [[Google Scholar](#)] [[Publisher Link](#)]
- [13] Yanyang Zeng et al., "Physical Layer Security for CRNs over Beaulieu-Xie Fading Channels," *Wireless Communications and Mobile Computing*, vol. 2022, pp. 1-9, 2022. [[CrossRef](#)] [[Google Scholar](#)] [[Publisher Link](#)]
- [14] Yunquan Dong, Pingyi Fan, and Khaled Ben Letaief, "High-Speed Railway Wireless Communications: Efficiency Versus Fairness," *IEEE Transactions on Vehicular Technology*, vol. 63, no. 2, pp. 925-930, 2014. [[CrossRef](#)] [[Google Scholar](#)] [[Publisher Link](#)]
- [15] Adebola Olutayo et al., "Level Crossing Rate and Average Fade Duration for the Beaulieu-Xie Fading Model," *IEEE Wireless Communications Letters*, vol. 6, no. 3, pp. 326-329, 2017. [[CrossRef](#)] [[Google Scholar](#)] [[Publisher Link](#)]
- [16] Veenu Kansal, and Simranjit Singh, "Analysis of Effective Capacity over Beaulieu-Xie Fading Model," *2017 IEEE International WIE Conference on Electrical and Computer Engineering (WIECON-ECE)*, Dehradun, India, pp. 207-210, 2017. [[CrossRef](#)] [[Google Scholar](#)] [[Publisher Link](#)]
- [17] Manpreet Kaur, and Rajesh Kumar Yadav, "Performance Analysis of Beaulieu-Xie Fading Channel with MRC Diversity Reception," *Transactions on Emerging Telecommunications Technology*, vol. 31, no. 7, 2020. [[CrossRef](#)] [[Google Scholar](#)] [[Publisher Link](#)]
- [18] Veenu Kansal, and Simranjit Singh, "Effective Rate Analysis of MISO over Beaulieu-Xie Fading Channel," *AEU - International Journal of Electronics and Communications*, vol. 138, 2021. [[CrossRef](#)] [[Google Scholar](#)] [[Publisher Link](#)]
- [19] Aleksey S. Gvozdev et al., "Reconfigurable Intelligent Surfaces' Impact on the Physical Layer Security of the Beaulieu-Xie Shadowed Fading Channel," *2022 International Symposium on Networks, Computers and Communications (ISNCC)*, Shenzhen, China, pp. 1-5, 2022. [[CrossRef](#)] [[Google Scholar](#)] [[Publisher Link](#)]
- [20] D. Krstic et al., "Outage Probability Determining for Wireless Systems in the Presence of Beaulieu-Xie Fading and Co-channel Interference Rayleigh Modeled," *2023 46<sup>th</sup> MIPRO ICT and Electronics Convention (MIPRO)*, Opatija, Croatia, pp. 523-526, 2023. [[CrossRef](#)] [[Google Scholar](#)] [[Publisher Link](#)]



- [21] Adebola Olutayo et al., “Performance of Wireless Powered Communication Systems over Beaulieu-Xie Channels with Nonlinear Energy Harvesters,” *IEEE Open Journal of the Communications Society*, vol 4, pp. 456-463, 2023. [[CrossRef](#)] [[Google Scholar](#)] [[Publisher Link](#)]
- [22] Hao Chen et al., “A Class of Low-Complexity Transmit Antenna Selection Schemes for Spatial Modulation,” *2024 IEEE 24<sup>th</sup> International Conference on Communication Technology (ICCT)*, Chengdu, China, pp. 2046-2050, 2024. [[CrossRef](#)] [[Google Scholar](#)] [[Publisher Link](#)]
- [23] Dang The Hung, Do Van Hung, and Le Trong Trung, “Performance Analysis of MIMO TAS/SC System in Short Packet Communication,” *2024 International Conference on Advanced Technologies for Communications (ATC)*, Ho Chi Minh City, Vietnam, pp. 911-916, 2024. [[CrossRef](#)] [[Google Scholar](#)] [[Publisher Link](#)]
- [24] Jia Li et al., “Secrecy Analysis in UAV-aided MIMO-NOMA Network with TAS/MRC Against Random Eavesdroppers,” *IEEE Internet of Things Journal*, pp. 1-1, 2025. [[CrossRef](#)] [[Google Scholar](#)] [[Publisher Link](#)]
- [25] Simon Marvin K., and Mohamed-Slim Alouini, *Digital Communication Over Fading Channels*, 2<sup>nd</sup> ed., John Wiley & Sons, 2004. [[Google Scholar](#)] [[Publisher Link](#)]
- [26] Yao Ma, R. Schober, and S. Pasupathy, “Effect of Channel Estimation Error on MRC Diversity in Rician Fading Channels,” *IEEE Transactions on Vehicular Technology*, vol 54, no. 6, pp. 2137-2142, 2005. [[CrossRef](#)] [[Google Scholar](#)] [[Publisher Link](#)]
- [27] Pawan Kumar, and P.R. Sahu, “Analysis of M-PSK with MRC Receiver over  $\kappa - \mu$  Fading Channels with Outdated CSI,” *IEEE Wireless Communications Letters*, vol. 3, no. 6, pp. 557-560, 2014. [[CrossRef](#)] [[Google Scholar](#)] [[Publisher Link](#)]
- [28] I.S. Gradshteyn, and I.M. Ryzhik, *Table of Integrals, Series, and Products*, 6<sup>th</sup> ed., Academic Press, 2014. [[Google Scholar](#)]
- [29] Milton Abramowitz, and Irene A. Stegun, *Handbook of Mathematical Functions with Formulas, Graphs, and Mathematical Tables*, 1948. [[Google Scholar](#)]
- [30] Nico M. Temme, “Computational Aspects of Incomplete Gamma Functions with Large Complex Parameters,” *Approximation and Computation: A Festschrift in Honor of Walter Gautschi*, vol. 119, pp. 551-562, 1994. [[CrossRef](#)] [[Google Scholar](#)] [[Publisher Link](#)]
- [31] Q.T. Zhang, “Outage Probability in Cellular Mobile Radio due to Nakagami Signal and Interferers with Arbitrary Parameters,” *IEEE Transactions on Vehicular Technology*, vol. 45, no. 2, pp. 364-372, 1996. [[CrossRef](#)] [[Google Scholar](#)] [[Publisher Link](#)]
- [32] Juan P. Pena-Martin, Juan M. Romero-Jerez, and Concepcion Tellez-Labao, “Performance of TAS/MRC Wireless Systems under Hoyt Fading Channels,” *IEEE Transactions on Wireless Communications*, vol. 12, no. 7, pp. 3350-3359, 2013. [[CrossRef](#)] [[Google Scholar](#)] [[Publisher Link](#)]
- [33] A. Annamalai, C. Tellambura, and V.K. Bhargava, “Equal-Gain Diversity Receiver Performance in Wireless Channels,” *IEEE Transactions on Communications*, vol. 48, no. 10, pp. 1732-1745, 2000. [[CrossRef](#)] [[Google Scholar](#)] [[Publisher Link](#)]
- [34] Andrea Goldsmith, *Wireless Communications*, Cambridge University Press, 2005. [[CrossRef](#)] [[Google Scholar](#)] [[Publisher Link](#)]
- [35] M.-S. Alouini, and A.J. Goldsmith, “Capacity of Rayleigh Fading Channels under Different Adaptive Transmission and Diversity-Combining Techniques,” *IEEE Transactions on Vehicular Technology*, vol. 48, no. 4, pp. 1165-1181, 1999. [[CrossRef](#)] [[Google Scholar](#)] [[Publisher Link](#)]